Sub-optical-cycle attosecond control of molecular ionization by using Fourier-synthesized laser fields

Hideki Ohmura and Naoaki Saito
National Institute of Advanced Industrial Science and Technology, Higashi 1-1-1, Tsukuba, Ibaraki 305-8565, Japan

(Received 21 January 2020; accepted 3 April 2020; published 27 April 2020)

We have investigated the combined positive and negative orientation-selected and yield-enhanced and -suppressed molecular tunneling ionization of carbon monoxide by dual-phase control of femtosecond Fourier-synthesized laser pulses. To investigate the role of each harmonic light, two types of experiments have been performed: (1) two-color experiments using Fourier-synthesized laser fields consisting of a fundamental light and its second or third harmonics and (2) three-color experiments using Fourier-synthesized laser fields consisting of a fundamental light and its second and third harmonics obtained by changing each relative phase difference independently. Positive and negative orientation-selected ionization is induced by the $\omega + 2\omega$ laser fields, and yield-enhanced and -suppressed ionization is induced mainly by $\omega + 3\omega$ laser fields. The Fourier-synthesized $\omega + 2\omega + 3\omega$ laser fields concurrently enhance both positive and negative orientation-selected and yield-enhanced and -suppressed molecular tunneling ionization. The mechanism is discussed in connection with the sub-optical-cycle interference control of the laser waveforms.

DOI: 10.1103/PhysRevA.101.043419

I. INTRODUCTION

According to Fourier-transformation theory, periodic arbitrary light waveforms can be synthesized with a superposition of a fundamental light and its harmonics [1–4]. Characteristic waveforms such as attosecond (1 as $= 10^{-18}$ s) pulse trains and continuous sawtooth, square, and triangle shapes can be synthesized. Such light-wave engineering enables us to control sub-optical-cycle dynamics of electrons in matter, which is especially prominent in the presence of intense (greater than 10^{13} W/cm^2) laser fields. Typical examples of suboptical dynamics of electrons have been observed in tunneling ionization (TI) and following high-order harmonic generation (HHG) [4,5]. After pioneering theoretical attempts considered sub-optical-cycle control [6–11], trajectory control of the electron in HHG induced by Fourier-synthesized laser fields has been proposed theoretically [12] and achieved experimentally [13,14].

The TI induced by intense laser fields occurs when the binding potential of an electron is distorted by the electric field of a laser so strongly that the wave function of the highest occupied electron penetrates the potential barrier and the electron is liberated from the binding potential [15–19]. Experimental studies have shown that TI is induced mainly in the suboptical cycle of the attosecond time region, when the amplitude of the electric field of the laser peaks because of a high-order nonlinear optical response [20–23]. This indicates that the shaping of sub-optical-cycle waveforms enables us to control the TI.

In the case of molecules, the molecular Ammosov-Delone-Krainov (ADK) model [24,25], which is a simple extension of the ADK model widely used for atoms [17], has revealed that the angular dependence of the TI rate between the electric-field vector and the molecular axis reflects the geometric structure of the highest occupied molecular orbital (HOMO) [24,25] because photoelectrons are preferentially removed via the tunneling process from the large-amplitude lobe of the HOMO along the opposite direction of the electric-field vector. As a consequence of the angular dependence of the TI rate between the electric-field vector and the molecular axis, molecules oriented in a certain direction can be selectively ionized in a randomly oriented gas-phase molecular ensemble, and the photofragment-emission pattern induced by molecular TI reflects the geometric structure of the HOMO [26,27]. Advanced theories that consider the Stark effect [28,29], orbital distortion in the presence of intense laser fields [30,31], and the multielectron effect [32] have been developed.

We have investigated sub-optical-cycle control of laser waveforms and resultant orientation-selected molecular TI induced by phase-controlled two-color laser fields consisting of a fundamental light and its second harmonics in various molecules [33–37]. Orientation-selected molecular TI that reflects the geometric structure of the HOMO has been observed in a broad range of molecules [33–37]. Recently, we have reported that directionally asymmetric TI induced by intense, nanosecond, three-color Fourier-synthesized laser fields led to four-mode selection with a combination of positive and negative orientation-selected and yield-enhanced and -suppressed molecular ionization of carbonyl sulfide [38]. The electric field of a linearly polarized Fourier-synthesized laser field consisting of a fundamental light and its harmonics (hereafter $\omega + 2\omega$, $\omega + 3\omega$ [two-color], and $\omega + 2\omega + 3\omega$ [three-color] laser fields) is given by $E(t) = E_1\cos(\omega t) + \Sigma^3{}_{n=2}E_n\cos(n\omega t + \phi_{1n})$, where the $E_n (n = 1, 2, 3)$ are the amplitudes of the electric field of each component ($\omega + 2\omega$; $E_3 = 0$, $\omega + 3\omega$; $E_2 = 0$), and $\phi_{1n} (n = 2, 3)$ are the relative phase differences between ω and its harmonic field. The mechanism of the four-mode selective ionization process has been discussed in connection with the waveforms of Fourier-synthesized laser fields. However, the details have not been sufficiently investigated, in part because we used an interferometer-free Fourier-synthesized laser field generator

[39]. The interferometer-free Fourier-synthesized laser field generator is stable for any phase fluctuations without fine adjustments, where the phase fluctuations in the fundamental and its harmonic beams cancel out when the beams pass along the same path, and both temporal and spatial overlaps of the fundamental and second-harmonic beams are ensured without optical adjustments. In practice, this method has enabled us to observe the phase-sensitive signals induced by the Fourier-synthesized laser fields with high stability and reproducibility. In this method, however, each beam is not separated spatially so that each ϕ_{1n} cannot be controlled independently. In this paper we adopted a multicolor Mach-Zehnder interferometer that can control the ϕ_{1n} of each beam independently, and we employed a femtosecond laser source and carbon monoxide (CO) as the targeted molecule to create more suitable conditions for TI [40]. We have performed two types of experiments to investigate the role of each harmonic light: (1) two-color experiments using $\omega + 2\omega$ and $\omega + 3\omega$ laser fields and (2) three-color experiments using Fourier-synthesized $\omega + 2\omega + 3\omega$ laser fields by changing each ϕ_{12} or ϕ_{13} independently to investigate the details of the independent phase-sensitive signals as a function of each ϕ_{12} or ϕ_{13}. A characteristic difference between ϕ_{12} dependence and ϕ_{13} dependence was observed as inverted and noninverted orientation-selected molecular ionization.

II. EXPERIMENT

The experimental apparatus was composed of a Ti:sapphire laser system, a multicolor Mach-Zehnder interferometer generating Fourier-synthesized laser fields [40], and a time-of-flight mass spectrometer (TOF-MS) equipped with a supersonic molecular-beam source. The Ti:sapphire laser (Spectra-Physics, Hurricane) generated horizontally polarized, 130-fs-duration laser pulses at a 800-nm wavelength and was operated at a repetition rate of 10 Hz. The 800-nm (ω) pulses were converted to 400-nm (2ω) pulses by a frequency doubling crystal [β-barium borate (BBO), type-I phase matching, 0.5-mm thickness, 40% conversion efficiency]. After the ω and 2ω pulses passed through a calcite plate for group velocity delay compensation and a dual wave plate ($\lambda/2$ retardation for the ω pulse and λ retardation for the 2ω pulse), the $\omega + 2\omega$ pulses were converted to 266-nm (3ω) pulses by a BBO crystal (type-I phase matching, 0.1-mm thickness, 20% conversion efficiency) via sum frequency generation ($\omega + 2\omega \rightarrow 3\omega$).

Each harmonic light was separated from the fundamental light by dielectric mirrors in the multicolor Mach-Zehnder interferometer, which is described in a previous report (three arms of the four-arm interferometer were used) [40]. Each ϕ_{1n} was controlled by changing the optical path length of each harmonic light by using a translation stage driven by a piezoelectric actuator with a resolution of about 2 nm. The polarizations of the three laser fields were set to be parallel by using a half-wave plate for the 3ω pulses. The spatial and temporal overlapping between the fundamental and harmonic beams were checked by the technique we described previously [40]. After being recombined, the Fourier-synthesized $\omega + 2\omega + 3\omega$ beams were introduced to the TOF-MS and were focused on the molecular beam by a concave mirror (200-mm focal length). The total intensity $I = I_1 + I_2 + I_3$ was $5 \times 10^{13}\,\mathrm{W/cm^2}$ at the focus, and the ratios I_2/I_1 and I_3/I_1 were around 0.4 and 0.1, respectively, where I_1, I_2, and I_3 are the intensities of the ω, 2ω, and 3ω pulses. The ratios I_2/I_1 and I_3/I_1 were adjusted by slightly rotating the phase-matching angle of the BBO while keeping the total intensity I constant. We verified that the ionization yield induced by only 3ω pulses is less than 5% of the total ionization yield induced by three-color Fourier-synthesized laser pulses; thus, the contribution to multiphoton ionization by only 3ω pulses is negligible.

A TOF-MS equipped with a pulsed supersonic molecular-beam source was used to detect the ionized molecules and their photofragments. The target gas for the molecular beam was diluted (5%) with helium gas to obtain a total pressure of $1.0 \times 10^5\,\mathrm{Pa}$. By operating the pulsed molecular beam at 10 Hz, the pressure in the TOF-MS was kept below $2.0 \times 10^{-5}\,\mathrm{Pa}$. Molecular ions and their photofragment ions generated by the Fourier-synthesized laser pulses were detected with a microchannel plate detector. TOF spectra were recorded with a digital oscilloscope.

The polarization direction of the $\omega + 2\omega + 3\omega$ laser fields was set to be parallel to the TOF axis. We defined the positive direction for $E(t)$ as the direction pointing to the ion detector, so that $\phi_{12} = \phi_{13} = 0$ when the electric-field maxima pointed in the positive direction (forward-backward configuration in Ref. [36]).

III. RESULTS AND DISCUSSIONS

We selected CO as the molecular model for this paper because the TI of CO molecules has been investigated theoretically [29,30,32,41,42] and experimentally [36,43,44]. Some experimental reports showed that the geometric structure of the HOMO (5σ orbital) dominates the orientation-dependent TI of CO, where photoelectrons are preferentially removed from the large amplitude lobe of the HOMO (carbon side) along the opposite direction of the electric-field vector [36,43,44].

Two types of experiments have been performed to investigate the role of each harmonic light in the Fourier-synthesized laser fields: (1) two-color experiments using $\omega + 2\omega$ laser fields and $\omega + 3\omega$ laser fields and (2) three-color experiments using Fourier-synthesized $\omega + 2\omega + 3\omega$ laser fields by changing each ϕ_{12} or ϕ_{13} independently. We have previously reported on an experiment using $\omega + 2\omega$ laser fields [36]. Figure 2 of Ref. [36] shows the TOF spectra of single-charged C^+ and O^+ ions produced when CO molecules were irradiated with $\omega + 2\omega$ laser fields at (a) $\phi_{12} = 0$ and (b) $\phi_{12} = \pi$. Each photofragment was observed as a pair of peaks, the first peak resulting from ions ejected directly toward the detector and the second from ions that were first ejected in the backward direction before being accelerated toward the detector by the extraction field. The characteristic breaking of the forward-backward symmetry was clearly observed in the TOF spectra. The backward peak of the C^+ ions predominated, and the forward peak of the O^+ ions predominated at $\phi_{12} = 0$. This forward-backward asymmetry was reversed at $\phi_{12} = \pi$. These results show that dissociative ionization was induced by the $\omega + 2\omega$ laser fields while discriminating between head or tail orientation of the molecule. We defined positive orientation of

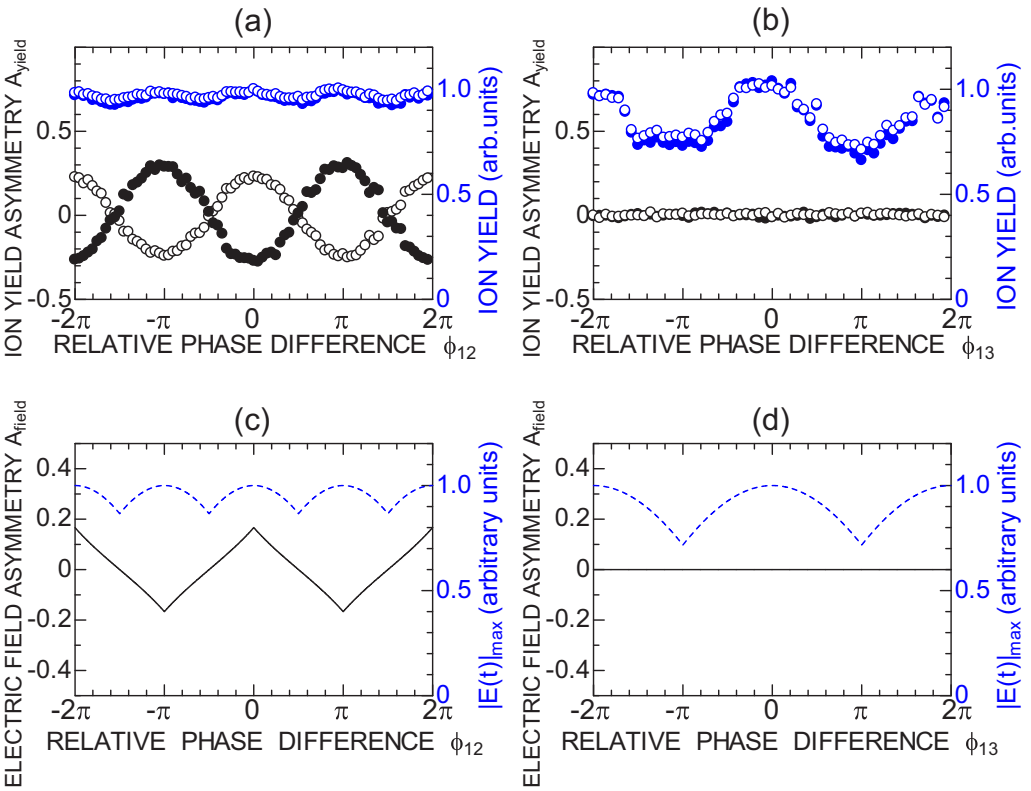

FIG. 1. (a, b) Left axis, black symbols: Ion yield asymmetry of photofragment ions $A_{\text{yield}} = (I_F - I_B)/(I_F + I_B)$ as a function of (a) ϕ_{12} for $\omega + 2\omega$ laser fields and (b) ϕ_{13} for $\omega + 3\omega$ laser fields: open circles, C^+ photofragment ions; closed circles, O^+ photofragment ions. Right axis, blue symbols: Total yield of photofragment ions $I_{\text{total}} = I_F + I_B$ as a function of (a) ϕ_{12} for $\omega + 2\omega$ laser fields and (b) ϕ_{13} for $\omega + 3\omega$ laser fields: open circles, C^+ photofragment ions; closed circles, O^+ photofragment ions. (c, d) Left axis, black solid curves: Electric-field asymmetry A_{field} as a function of (c) ϕ_{12} for $\omega + 2\omega$ laser fields and (d) ϕ_{13} for $\omega + 3\omega$ laser fields. Right axis, blue dotted curves: Absolute values of the electric-field maxima $|E(t)|_{\text{max}}$ as a function of (c) ϕ_{12} for $\omega + 2\omega$ laser fields and (d) ϕ_{13} for $\omega + 3\omega$ laser fields ($E_2/E_1 = 1/2$, $E_3/E_1 = 1/2$).

a molecule as the configuration of the molecule in which the O atom points toward the ion detector.

We first analyzed the phase dependence of the C^+ and O^+ photofragment ions in the two-color experiments to understand the behavior of the phase-dependent photofragment ions. We defined the ion yield asymmetry A_{yield} of the photofragment ions to be $(I_F - I_B)/(I_F + I_B)$, where $I_F(I_B)$ is the signal intensity of the forward (backward) photofragment emission. Figures 1(a) and 1(b) depict A_{yield} for (a) $\omega + 2\omega$ laser fields as a function of ϕ_{12} and (b) $\omega + 3\omega$ laser fields as a function of ϕ_{13}. Clear sinusoidal patterns of A_{yield} were observed in C^+ and O^+ for $\omega + 2\omega$ laser fields, and the A_{yield} values of the C^+ and O^+ ions were completely out of phase with each other [Fig. 1(a)]. These results show that Fourier-synthesized $\omega + 2\omega$ fields can distinguish between head and tail orientations of a molecule, and the orientation is inverted between $\phi_{12} = 0$ and $\pm\pi$. In contrast, the behavior of A_{yield} as a function of ϕ_{13} for $\omega + 3\omega$ laser fields showed no phase dependence [Fig. 1(b)]. These results show that $\omega + 3\omega$ fields do not have the capability of orientation-selected molecular ionization.

Something about the complexity of monitoring the TI through dissociative ionization channels should be noted. The dissociative ionization processes include several entangled processes such as (1) direct dissociative ionization of CO by removing the electron from the HOMO, i.e., the ionization directly terminates in the dissociation continuum of the ion's electronic ground state (direct process), and (2) indirect dissociative ionization with the first step being tunneling ionization removing an electron from the CO HOMO and leaving the ion in the electronic ground state in bound vibrational levels followed by further excitation of the ion to excited electronic states which then terminate in dissociation of the ion (indirect process). It seems the direct process to be suppressed compared to the indirect one. The potential-energy curves of the electronic ground states of CO and CO^+ seem to be not too different since the equilibrium internuclear separations are very close and the vibrational constants very similar. Thus, the Franck-Condon factor for direct excitation from the CO vibrational ground state to the dissociation continuum of the electronic ground state of CO^+ is probably very small, therefore suppressing the direct dissociative ionization pathway relative to the indirect one. Although we cannot distinguish the direct process from the stepwise process in our experiments, the dissociation process should have certain contributions such as charge localization, which result in asymmetries of photofragment ions [45]. If charge localization is considered, the ion yield asymmetries of the C^+ and O^+ ions are expected to be in phase with each other. Furthermore, the phase dependences of fragment ions

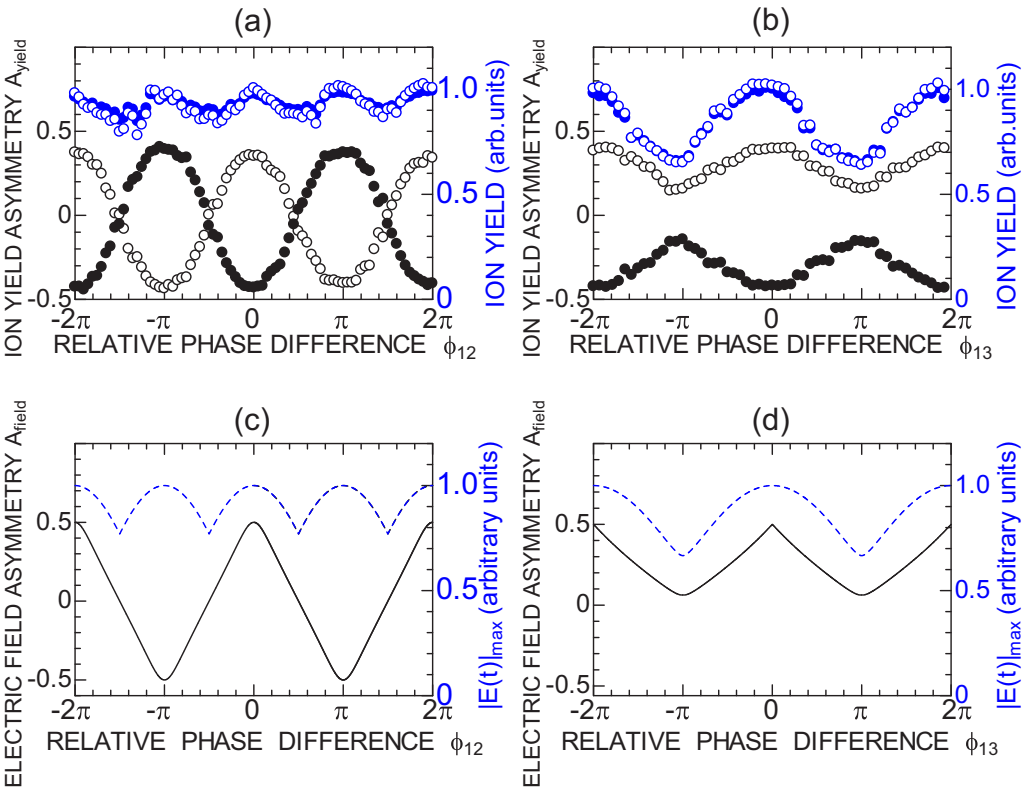

FIG. 2. (a, b) Left axis, black symbols: Ion yield asymmetry of photofragment ions $A_{\rm yield} = (I_{\rm F} - I_{\rm B})/(I_{\rm F} + I_{\rm B})$ as a function of (a) ϕ_{12} with $\phi_{13} = 0$ and (b) ϕ_{13} with $\phi_{12} = 0$ for $\omega + 2\omega + 3\omega$ laser fields: open circles, C^+ photofragment ions; closed circles, O^+ photofragment ions. Right axis, blue symbols: Total yield of photofragment ions $I_{\rm total} = I_{\rm F} + I_{\rm B}$ as a function of (a) ϕ_{12} with $\phi_{13} = 0$ and (b) ϕ_{13} with $\phi_{12} = 0$ for $\omega + 2\omega + 3\omega$ laser fields: open circles, C^+ photofragment ions; closed circles, O^+ photofragment ions. (c, d) Left axis, black solid curves: Electric-field asymmetry $A_{\rm field}$ as a function of (c) ϕ_{12} with $\phi_{13} = 0$ and (d) ϕ_{13} with $\phi_{12} = 0$ for $\omega + 2\omega + 3\omega$ laser fields. Right axis, blue dotted curves: Absolute values of the electric-field maxima $|E(t)|_{\rm max}$ as a function of (c) ϕ_{12} with $\phi_{13} = 0$ and (d) ϕ_{13} with $\phi_{12} = 0$ for $\omega + 2\omega + 3\omega$ laser fields ($E_2/E_1 = 2/3, E_3/E_1 = 1/3$).

were reported to be dependent on their kinetic energies [46]. In our experimental results, the ion yield asymmetries of the C^+ and O^+ ions were completely out of phase with each other, and the phase dependences of fragment ions were not dependent on their kinetic energies. These results show that CO molecules are orientation-selectively ionized in the first TI process; the other processes that follow that contribute to ion yield asymmetries are washed away, causing other effects that induce ion yield asymmetries to appear to be minor. Therefore, we conclude that the main contribution that dominates the phase dependence of fragment ion emission is the first TI process. We also note the possibility of electron removal from orbitals other than HOMO. If parent ions generated by electron removal from the HOMO via TI are not directly or stepwise connected to dissociation channels and the observed photofragment ions are generated via dissociation channels connected to orbitals other than the HOMO, the direction of the orientation-selectively ionized molecules could differ from that expected by the shape of the HOMO [47]. In this paper, the total intensity of the Fourier-synthesized laser fields is $5 \times 10^{13}\,{\rm W/cm^2}$. This laser intensity is strong enough for CO molecules to induce TI from the HOMO but not so strong as to induce TI from inner orbitals such as HOMO-1. Since the direction of the oriented molecules is consistent with that expected by the shape of the HOMO, it is reasonable to conclude that TI from the HOMO is the main contribution.

Furthermore, we analyzed the phase dependence of the total yield $I_{\rm total}(= I_{\rm F} + I_{\rm B})$ for the C^+ and O^+ photofragment ions to understand the mechanism of the yield-enhanced and -suppressed molecular ionization processes. Figures 1(a) and 1(b) also depict $I_{\rm total}$ for (a) $\omega + 2\omega$ laser fields as a function of ϕ_{12} and (b) $\omega + 3\omega$ laser fields as a function of ϕ_{13}. Slight phase-dependent behavior of $I_{\rm total}$ with π periodicity was observed in the case of $\omega + 2\omega$ laser fields for C^+ and O^+ [Fig. 1(a)]. In contrast, large periodic enhancement and suppression of $I_{\rm total}$ with 2π periodicity were clearly observed in the case of $\omega + 3\omega$ laser fields for C^+ and O^+ [Fig. 1(b)]. From these results we conclude that positive and negative orientation-selected TI is induced by $\omega + 2\omega$ laser fields, and yield-enhanced and -suppressed TI is induced mainly by $\omega + 3\omega$ laser fields. We note that the $I_{\rm total}$ values of C^+ and O^+ were in phase with each other, so that there was no phase dependence of the branching ratio of the two reaction pathways: $CO^+ \rightarrow C^+ + O$ or $C + O^+$.

Next, we analyzed the phase dependence of the C^+ and O^+ photofragment ions for Fourier-synthesized $\omega + 2\omega + 3\omega$ laser fields. Figure 2 depicts $A_{\rm yield}$ for $\omega + 2\omega + 3\omega$ laser fields as a function of (a) ϕ_{12} with $\phi_{13} = 0$ and (b) ϕ_{13}

with $\phi_{12} = 0$. Clear periodicities of 2π were observed in A_{yield} as a function of ϕ_{12} and ϕ_{13} for both C^+ and O^+ [Figs. 2(a) and 2(b)]. Both phase dependencies of C^+ and O^+ were completely out of phase with each other. The ϕ_{12} dependencies of C^+ and O^+ crossed each other. On the other hand, the ϕ_{13} dependencies of C^+ and O^+ anticrossed each other. (This discrepancy is discussed below.) These results show that CO molecules are orientation-selectively ionized while discriminating the head and tail orientation of the molecules by Fourier-synthesized $\omega + 2\omega + 3\omega$ laser fields. The out-of-phase behavior with crossing between C^+ and O^+ in the ϕ_{12} dependence of A_{yield} shows that the orientation of ionized molecules is inverted between $\phi_{12} = 0$ and $\pm\pi$. In contrast, the out-of-phase behavior with anticrossing between C^+ and O^+ in the ϕ_{13} dependence of A_{yield} indicates that CO molecules are orientation-selectively ionized, but their orientation is not inverted between $\phi_{12} = 0$ and $\pm\pi$. As shown in Figs. 2(a) and 2(b), the maximum amplitude of A_{yield} is enhanced by adding 3ω laser pulses.

Figures 2(a) and 2(b) depict I_{total} for $\omega + 2\omega + 3\omega$ laser fields as a function of (a) ϕ_{12} with $\phi_{13} = 0$ and (b) ϕ_{13} with $\phi_{12} = 0$. Clearer ϕ_{12}-dependent behavior of I_{total} with π periodicity was observed than in the case of $\omega + 2\omega$ laser fields for C^+ and O^+ [Fig. 2(a)]. Furthermore, large ϕ_{13}-dependent enhancement and suppression of I_{total} with 2π periodicity were apparent in the case of $\omega + 2\omega + 3\omega$ laser fields for C^+ and O^+ [Fig. 2(b)]. From these results, we conclude that Fourier-synthesized $\omega + 2\omega + 3\omega$ laser fields concurrently enhance both positive and negative orientation-selected and yield-enhanced and -suppressed molecular tunneling ionization.

To elucidate the mechanism that accounts for positive and negative orientation-selected, yield-enhanced and -suppressed molecular TI, we calculated the two phase-dependent characteristics of the electric field that could affect molecular TI: the absolute value of the maxima of the electric-field amplitude, $|E(t)|_{\max}$, and the electric-field asymmetry, A_{field}, defined by $A_{\text{field}} = [|E(t)_{\max}| - |E(t)_{\min}|]/[|E(t)_{\max}| + |E(t)_{\min}|]$ [39]. The maximum (minimum) of $|E(t)|_{\max}$ can be connected to enhancement (suppression) of the yield of molecular TI. A_{field} weighs the difference between the positive and negative amplitudes of the electric field. When TI occurs in molecules with an asymmetric structure, the TI rates are expected to differ between positively oriented and negatively oriented molecules. As a result, the asymmetric waveform of the Fourier-synthesized laser field can selectively ionize molecules while discriminating between head and tail orientation of molecules with asymmetric structures [33–37]. This selectivity and discrimination cannot be achieved by single-frequency laser fields with symmetric waveforms.

The solid lines of Figs. 1(c) and 1(d) depict the field asymmetry A_{field} as a function of ϕ_{12} for $\omega + 2\omega$ laser fields [Fig. 1(c)] and as a function of ϕ_{13} for $\omega + 3\omega$ laser fields [Fig. 1(d)]. A_{field} is inverted between $\phi_{12} = 0$ and $\pm\pi$ for $\omega + 2\omega$ laser fields. On the other hand, A_{field} has no phase dependence with a value of zero for $\omega + 3\omega$ laser fields. This means that $\omega + 3\omega$ laser fields have symmetric waveforms with respect to positive and negative directions so that $\omega + 3\omega$ laser fields do not have the capability of orientation-selected ionization while discriminating between head and tail orientation of molecules with asymmetric structures [33–37]. This behavior is consistent with the experimental results of orientation-selected ionization.

The dotted lines of Figs. 1(c) and 1(d) show the value of $|E(t)|_{\max}$ as a function of ϕ_{12} for $\omega + 2\omega$ laser fields [Fig. 1(c)] and as a function of ϕ_{13} for $\omega + 3\omega$ laser fields [Fig. 1(d)]. They reach maxima (minima) at $\phi_{12} = 0, \pm\pi$ ($\pm\pi/2, \pm 3\pi/2$) [Fig. 1(c)]. On the other hand, they reach maxima (minima) at $\phi_{13} = 0$ ($\pm\pi$) [Fig. 1(d)]. These maxima and minima are consistent with the experimental results of enhancement (suppression) of the yield of molecular TI.

Similarly, we calculated A_{field} and $|E(t)|_{\max}$ for three-color Fourier-synthesized $\omega + 2\omega + 3\omega$ laser fields. The solid lines of Figs. 2(c) and 2(d) show the value of A_{field} as a function of ϕ_{12} with $\phi_{13} = 0$ [Fig. 2(c)] and ϕ_{13} with $\phi_{12} = 0$ [Fig. 2(d)] for Fourier-synthesized $\omega + 2\omega + 3\omega$ laser fields. A_{field} as a function of ϕ_{12} is inverted between $\phi_{12} = 0$ and $\pm\pi$ for $\omega + 2\omega + 3\omega$ laser fields. More importantly, compared to two-color laser fields, the contrast of phase-dependent behavior is also enhanced. This behavior is consistent with the experimental results of orientation-selected ionization for three-color Fourier-synthesized laser fields. On the other hand, A_{field} as a function of ϕ_{13} is not inverted between $\phi_{12} = 0$ and $\pm\pi$ for $\omega + 2\omega + 3\omega$ laser fields. This means that $\omega + 2\omega + 3\omega$ laser fields lead to orientation-selected ionization, but the orientation is not inverted by ϕ_{13}. This behavior is also consistent with the experimental results of orientation-selected ionization.

The dotted lines of Figs. 2(c) and 2(d) show the value of $|E(t)|_{\max}$ as a function of ϕ_{12} with $\phi_{13} = 0$ [Fig. 2(c)] and ϕ_{13} with $\phi_{12} = 0$ [Fig. 2(d)] for $\omega + 2\omega + 3\omega$ laser fields. They reach maxima (minima) at $\phi_{12} = 0, \pm\pi$ ($\pm\pi/2, \pm 3\pi/2$) [Fig. 2(c)]. On the other hand, they reach maxima (minima) at $\phi_{13} = 0$ ($\pm\pi$) [Fig. 2(d)]. More importantly, compared to the case of two-color laser fields, the contrast of phase-dependent behavior in $|E(t)|_{\max}$ is enhanced. These maxima and minima are also consistent with the experimental results of yield-enhanced and -suppressed ionization.

Figure 3 illustrates the visualized relation between waveforms of Fourier-synthesized three-color $\omega + 2\omega + 3\omega$ laser fields and the direction of orientation-selectively ionized molecules. The waveforms of Fourier-synthesized three-color $\omega + 2\omega + 3\omega$ laser fields at relative phase differences $(\phi_{12}, \phi_{13}) = (0, 0), (\pi, 0)$ show maximum amplitudes and field asymmetries in the positive (0, 0) and negative (π, 0) directions, respectively, due to constructive interference among three-color laser fields within the suboptical cycle, inducing positive and negative orientation-selected, yield-enhanced molecular TI. On the other hand, the waveforms of Fourier-synthesized three-color $\omega + 2\omega + 3\omega$ laser fields at relative phase difference $(\phi_{12}, \phi_{13}) = (0, \pi)$ show minimum amplitudes with less field asymmetry due to destructive interference among three-color laser fields within the suboptical cycle, inducing positive-orientation selected, yield-suppressed molecular TI. The addition of 3ω pulses allows fine suboptical interference control of not only the field asymmetry but also the maximum field amplitude.

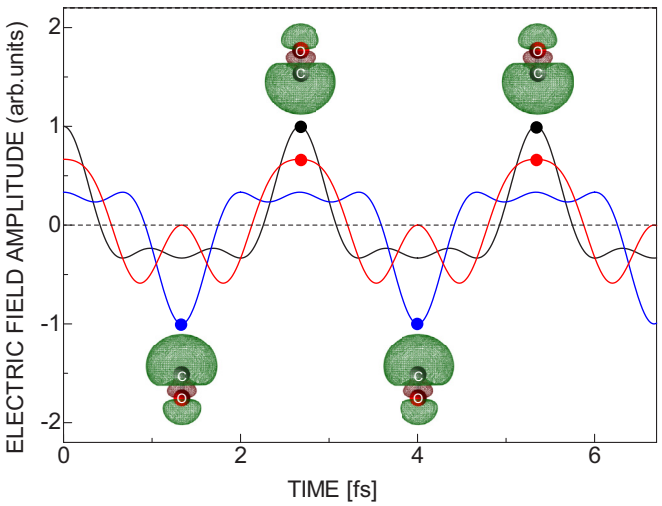

FIG. 3. Waveforms of Fourier-synthesized three-color $\omega + 2\omega + 3\omega$ laser fields at relative phase differences $(\phi_{12}, \phi_{13}) = (0, 0)$ (black curve), $(\pi, 0)$ (blue curve), and $(0, \pi)$ (red curve) $(E_2/E_1 = 2/3, E_3/E_1 = 1/3)$ and schematics of the molecular orientation and isocontours of the HOMO for orientation-selectively ionized CO. Closed dots indicate the points at maximum field amplitude.

IV. CONCLUSIONS

We have investigated the positive and negative orientation-selected and yield-enhanced and -suppressed molecular TI of carbon monoxide by dual-phase control of femtosecond Fourier-synthesized laser pulses. Positive and negative orientation-selected molecular TI is achieved by $\omega + 2\omega$ laser fields, whereas yield-enhanced and -suppressed TI is mainly achieved by $\omega + 3\omega$ laser fields. Fourier-synthesized $\omega + 2\omega + 3\omega$ laser fields concurrently enhance both positive and negative orientation-selected and yield-enhanced and -suppressed molecular TI. Fine suboptical interference control of three-color Fourier-synthesized laser fields provides control of both the field asymmetry and the maximum field amplitude, leading to positive and negative orientation-selected and yield-enhanced and -suppressed TI.

We have previously reported on four-mode selection with a combination of positive and negative orientation-selected and yield-enhanced and -suppressed molecular TI [38]. Orientation-selected and yield-enhanced molecular TI is easy to understand because maximum orientation selectivity always shows yield-enhanced ionization. However, orientation-selected yield-suppressed TI occurs when the orientation selectivity is not a maximum, suggesting that characteristic ionization is not always induced at relative phase differences with multiple integers or fractions of π. We emphasize that the observation of combined positive and negative orientation-selected and yield-enhanced and -suppressed molecular TI provides us with a way to characterize arbitrary light waveforms in terms of $|E(t)|_{\max}$ and A_{field}. The suppression of ionization while irradiating intense laser fields is a key to the control of HHG [12–14], because the efficiency of HHG, where photoelectrons are accelerated and recollided back to the ground states of atoms and molecules by intense laser fields within one optical cycle, is restricted by the depletion of ground-state atoms and molecules due to ionization. A measurement of both HHG while monitoring $|E(t)|_{\max}$ and A_{field} by using photofragment ions in asymmetric molecules has the possibility to maximize the efficiency and cutoff in HHG, leading to the efficient generation of coherent soft x rays by HHG.

ACKNOWLEDGMENTS

This work was supported by JSPS KAKENHI Grants No. 24340097, No. 16H04103, and by the TACMI (Technical Alliance for Cool laser Machining with Intelligence) project commissioned by the New Energy and Industrial Technology Development Organization (NEDO).

[1] T. W. Hänsch, Opt. Commum. **80**, 71 (1990).
[2] M. Y. Shverdin, D. R. Walker, D. D. Yavuz, G. Y. Yin, and S. E. Harris, Phys. Rev. Lett. **94**, 033904 (2005).
[3] H.-S. Chan, Z.-M. Hsieh, W.-H. Liang, A. H. Kung, C.-K Lee, C.-J. Lai, R.-P Pan, and L.-H. Peng, Science **331**, 1165 (2011).
[4] P. B. Corkum and F. Krausz, Nature Phys. **3**, 381 (2007), and references therein.
[5] F. Krausz and M. Ivanov, Rev. Mod. Phys. **81**, 163 (2009), and references therein.
[6] M. B. Gaarde, A. L'Huillier, and M. Lewenstein, Phys. Rev. A **54**, 4236 (1996).
[7] D. B. Milošević and B. Piraux, Phys. Rev. A **54**, 1522 (1996).
[8] W. Becker, B. N. Chichkov, and B. Wellegehausen, Phys. Rev. A **60**, 1721 (1999).
[9] C. Figueira de Morisson Faria, M. Dőrr, W. Becker, and W. Sandner, Phys. Rev. A **60**, 1377 (1999).
[10] C. Figueira de Morisson Faria, D. B. Milošević, and G. G. Paulus, Phys. Rev. A **61**, 063415 (2000).
[11] D. B. Milošević, W. Becker, and R. Kopold, Phys. Rev. A **61**, 063403 (2000).
[12] L. E. Chipperfield, J. S. Robinson, J. W. G. Tisch, and J. P. Marangos, Phys. Rev. Lett. **102**, 063003 (2009).
[13] P. Wei, J. Miao, Z. Zeng, C. Li, X. Ge, R. Li, and Z. Xu, Phys. Rev. Lett. **110**, 233903 (2013).
[14] S. Haessler, T. Balčiunas, G. Fan, G. Andriukaitis, A. Pugžlys, A. Baltuška, T. Witting, R. Squibb, A. Zaïr, J.W. G. Tisch, J. P. Marangos, and L. E. Chipperfield, Phys. Rev. X **4**, 021028 (2014).
[15] L. V. Keldysh, Zh. Eksp. Teor. Fiz. **47**, 1945 (1964) [Sov. Phys. JETP **20**, 1307 (1965)].
[16] A. M. Perelomov, N. B. Popov, and M. V. Terent'ev, Zh. Eksp. Teor. Fiz. **50**, 1393 (1966) [Sov. Phys. JETP **23**, 924 (1966)].
[17] M. V. Ammosov, N. B. Delone, and V. P. Krainov, Zh. Eksp. Teor. Fiz. **91**, 2008 (1986) [Sov. Phys. JETP **64**, 1191 (1986)].
[18] P. B. Corkum, N. H. Burnett, and F. Brunel, Phys. Rev. Lett. **62**, 1259 (1989).
[19] E. Mevel, P. Breger, R. Trainham, G. Petite, P. Agostini, A. Migus, J.-P. Chambaret, and A. Antonetti, Phys. Rev. Lett. **70**, 406 (1993).

[20] M. Uiberacker, Th. Uphues, M. Schultze, A. J. Verhoef, V. Yakovlev, M. F. Kling, J. Raushenberger, N. M. Kabachnik, H. Schröder, M. Lezius, K. L. Kompa, H.-G. Muller, M. J. J. Vrakking, S. Hendel, U. Kleineberg, U. Heinzmann, M. Drescher, and F. Krausz, Nature (London) **446**, 627 (2007).
[21] P. Eckle, A. N. Pfeiffer, C. Cirelli, A. Staudte, R. Dörner, H. G. Muller, M. Büttiker, and U. Keller, Science **322**, 1525 (2008).
[22] A. Pfeiffer,C. Cirelli, M. Smolarski, D. Dimitrovski, M. Abu-samha, L. B. Madsen, and U. Keller, Nat. Phys. **8**, 76 (2012).
[23] U. S. Sainadh, H. Xu, X. Wang, A. Atia-tul-Noor, W. C. Wallace, N. Douguet, A. Bray, I. Ivanov, K. Bartschat, A. Kheifets, R. T. Sang, and I. V. Litvinyuk, Nature (London) **568**, 75 (2019).
[24] X. M. Tong, Z. X. Zhao, and C. D. Lin, Phys. Rev. A **66**, 033402 (2002).
[25] C. D. Lin and X. M. Tong, J. Photochem. Photobio. A **182**, 213 (2006).
[26] A. S. Alnaser, S. Voss, X.–M. Tong, C. M. Maharjan, P. Ranitovic, B. Ulrich, T. Osipov, B. Shan, Z. Chang, and C. L. Cocke, Phys. Rev. Lett. **93**, 113003 (2004).
[27] D. Pavičić, K. F. Lee, D. M. Rayner, P. B. Corkum, and D. M. Villeneuve, Phys. Rev. Lett. **98**, 243001 (2007).
[28] L. Holmegaard, J. K Hansen, L. Kalhøj, S. L. Kragh, H. Stapelfeldt, F. Filsinger, J. Küpper, G. Meijer, D Dimitrovski, M. Abu-samha, C. P. J. Martiny, and L. B. Madsen, Nat. Phys. **6**, 428 (2010).
[29] L. B. Madsen, F. Jensen, and O. I. Tolstikhin, and T. Morishita Phys. Rev. A **87**, 013406 (2013).
[30] M. D. Śpiewanowski and L. B. Madsen, Phys. Rev. A **91**, 043406 (2015).
[31] H. Akagi, T. Otobe, and R. Itakura, Sci. Adv. **5**, eaaw1885 (2019).
[32] B. Zhang, J. Yuan, and Z. Zhao, Phys. Rev. Lett. **111**, 163001 (2013).
[33] H. Ohmura, N. Saito, and M. Tachiya, Phys. Rev. Lett. **96**, 173001 (2006).
[34] H. Ohmura, F. Ito, and M. Tachiya, Phys. Rev. A **74**, 043410 (2006).
[35] H. Ohmura and M. Tachiya, Phys. Rev. A **77**, 023408 (2008).
[36] H. Ohmura, N. Saito, and T. Morishita, Phys. Rev. A **83**, 063407 (2011).
[37] H. Ohmura, N. Saito, and T. Morishita, Phys. Rev. A **89**, 013405 (2014).
[38] H. Ohmura, T. Yoshida, and N. Saito, Appl. Phys. Lett. **114**, 054101(2019).
[39] T. Yoshida, N. Saito, and H. Ohmura, J. Phys. B **51**, 065601 (2018).
[40] H. Ohmura and N. Saito, Phys. Rev. A **92**, 053408 (2015).
[41] V. P. Majety and A. Scrinzi, J. Phys. B **48**, 245603 (2015).
[42] S. Ohmura, T. Kato, T. Oyamada, S. Koseki, H. Ohmura, and H. Kono, J. Phys. B **51**, 034001 (2018).
[43] H. Li, D. Ray, S. De, I. Znakovskaya, W. Cao, G. Laurent, Z. Wang, M. F. Kling, A. T. Le, and C. L. Cocke, Phys. Rev. A **84**, 043429 (2011).
[44] J. Wu, L. Ph. H. Schmidt, M. Kunitski, M. Mecke, S. Voss, H. Sann, H. Kim, T. Jahnke, A. Czasch, and R. Dörner, Phys. Rev. Lett. **108**, 183001 (2012).
[45] M. F. Kling, Ch. Siedschlag, A. J. Verhoef, J. I. Khan, M. Schultze, Th. Uphues, Y. Ni, M. Uiberacker, M. Drescher, F. Krausz, and M. J. J. Vrakking, Science **312**, 246 (2006).
[46] Q. Song, Z. Li, S. Cui, P. Lu, X. Gong, Q. Ji, K. Lin, W. Zhang, J. Ma, H. Pan, J. Ding, M. F. Kling, H. Zeng, F. He, and J. Wu, Phys. Rev. A **94**, 053419 (2016).
[47] H. Akagi, T. Otobe, A. Staudte, A. Shiner, F. Turner, R. Dörner, D. M. Villeneuve, and P. B. Corkum, Science **325**, 1364 (2009).